

High-resolution, high-sensitivity ac calorimeter

Grzegorz Bednarz

Department of Physics, Dalhousie University, Halifax, Nova Scotia, B3H 4J5, Canada

Brian Millier

Department of Chemistry, Dalhousie University, Halifax, Nova Scotia, B3H 4J5, Canada

Mary Anne White^{a)}

Department of Physics and Department of Chemistry, Dalhousie University, Halifax, Nova Scotia, B3H 4J5, Canada

(Received 30 December 1991; accepted for publication 29 April 1992)

A high-resolution, high-sensitivity, automated ac calorimeter capable of heat capacity measurements on very small samples ($m < 20$ mg) with a temperature resolution of a few mK in the ac mode is described. This calorimeter also can be operated in the relaxation mode to provide absolute heat capacity values with precision and accuracy of around 2%. A microprocessor was employed to generate a stable oscillatory heating signal and to control the heater power, in order to improve the sensitivity of the measurement over other designs. A new very sensitive and miniature temperature probe (a film flake of a thermistor material), which increased measurement resolution and minimized the heat contribution of the addenda, also was used. This calorimeter was tested by measuring the heat capacity of gadolinium over its ferromagnetic phase transition. The results agree well with the literature data giving, however, substantially better resolution of the heat capacity in the critical region.

I. INTRODUCTION

Calorimetry is one of the oldest and the most extensively used research methods. Heat capacity data have a wide range of utility; they are used to determine various thermodynamic quantities and to reveal and characterize phase transitions.¹ The progress made in the physics of critical phenomena in the two decades since Wilson² formulated the renormalization group (R.G.) approach to phase transitions in 1971, has created a need for data giving the temperature dependence of the heat capacity, $C(T)$, at temperatures extremely close to the critical value, T_c . The required heat capacity resolution can be of the order of a few mK, in order to give reduced temperatures less than 10^{-3} . Despite impressive theoretical advances there are still few high-resolution experimental data sets available for the critical behavior of heat capacity for various systems (particularly for phase transitions in magnetic systems³). The available critical behavior data often are not suitable for R.G. analysis because they lack sufficient resolution around the critical temperature.⁴

The commonly used and well-known calorimetric methods are not very suited to high-resolution measurements. Adiabatic calorimetry, based on the heat-pulse method, is considered to be one of the most accurate calorimetric methods,⁵ but its precision drops dramatically for very small temperature increments. This method, however, has been used successfully for high-resolution heat capacity studies at very low temperatures, when heat loss by radiation becomes negligible,⁶ and digital measurement techniques have led to improvement of the precision of the heat-pulse method.⁷ Differential scanning calorimetry can

be quite sensitive but it also lacks resolution and accuracy due to its nonequilibrium nature.^{8,9}

There have been several ingenious methods of high-resolution heat capacity measurement. For example, in a continuous warming calorimeter,¹⁰ a thermally isolated sample was heated at a constant power and the heater capacity was derived from the rate of temperature increase. The principal source of error in this method is the uncertainty involved in determination of the temperature drift rate, which can be of the order of the actual drift rate for the temperature drift rates in mK range.

Another method appropriate for high-resolution measurements is the relaxation time method.¹¹ In this method, the sample temperature is increased, and then the heat is turned off and the temperature relaxation is recorded. The heat capacity is determined from this and from the experimentally determined heat conduction between the sample and its surroundings. This method was used in our work to calibrate the measurements made in the ac mode; it is described in more detail later.

In 1968 Sullivan and Seidel¹² introduced a new method of measuring heat capacity which has subsequently been called "ac calorimetry." This method has been used in the study of phase transitions in solids,^{13,14} liquid crystals and fluids,¹⁴ and biological materials.¹⁵ ac calorimetry offers very high (mK) resolution coupled with high sensitivity. This arises from the fact that this method measures amplitudes of periodic, mK temperature waves propagated through the sample. The changes in the temperature wave amplitude, which are caused by heat capacity variations with temperature, can be very accurately measured with a lock-in amplifier. Advances in materials science and electronics have allowed the application of ac calorimetry to extremely small samples ($m \approx 25$ μ g) (Ref. 16) and noisy environments.¹⁷

^{a)} Author to whom correspondence may be addressed.

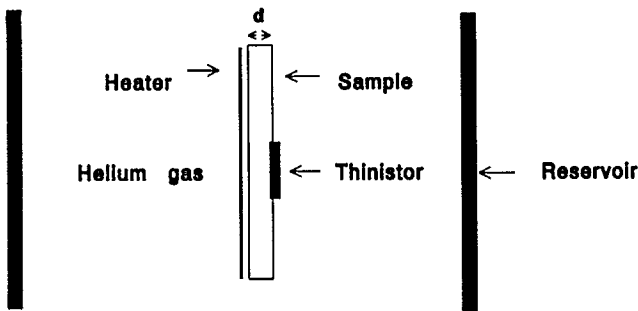


FIG. 1. Idealized one-dimensional heat flow problem.

In this paper we report the design and the construction of an ac calorimeter for the study of phase transitions in solids. This calorimeter also can be operated in the relaxation mode to give absolute values of heat capacity. In the following sections we describe the theory of ac calorimetry and relaxation-time calorimetry. The design of the electronics, which is crucial for the resolution in our calorimeter and which also allows relaxation mode measurements, is described in detail. We also describe in detail the designs of the cryostat and the sample assembly. Emphasis is put on the design of the sample heater and on the choice of the temperature probe, which allowed high-resolution heat capacity measurements while minimizing the heat capacity contribution of the addenda.

II. THEORY OF ac CALORIMETRY

The theory of ac calorimetry has been discussed extensively in a number of publications^{12,18,19} and theses.^{20,21} Therefore we give here only a brief review of the theory pertinent to the experimental geometry of our apparatus.

In the simplified model of an ac experiment shown in Fig. 1 the sample is a thin slice of material of uniform thickness d with a resistive heater attached to one face and a temperature sensor to the other. It is loosely thermally coupled to the reservoir at temperature T_0 via exchange gas and leads. The thermal conductance of this thermal link is K and the heat capacity of the sample assembly is C . If the sample assembly has infinite thermal conductivity and the thermal link has zero heat capacity, then the difference in temperature of the sample and the reservoir is given by Newton's law of cooling,

$$C\Delta\dot{T}(t) = P(t) - K\Delta T(t), \quad (1)$$

where $\Delta T(t)$ is the temperature difference between the sample and the reservoir and $P(t)$ is the heater power.

For a phase-sensitive detection at the second harmonic the oscillatory power used is $P(t) = P_0 \cos^2 \omega t$ and the steady-state solution to Eq. (1) can be written in the form:

$$\Delta T \approx \frac{P_0}{2K} + \frac{P_0}{4\omega C} \cos(2\omega t - \phi) = \Delta T_{dc} + \Delta T_{ac} \cos(2\omega t - \phi), \quad (2)$$

where ΔT_{dc} is the constant temperature difference between the sample and the heat sink and ΔT_{ac} is the amplitude of the ac oscillations, provided that $(\omega\tau)^2 \gg 1$, where $\tau = C/K$

is the external relaxation time and ϕ is the phase shift ($\tan \phi = 2\omega\tau$, $\phi \approx \pi/2$). A lock-in amplifier detects the second harmonic of the temperature oscillation which is inversely proportional to C . Detection at the second harmonic is useful because of a built-in advantage of discrimination against leakage from the heater voltage.

In a real system two time constants characterize the thermal dynamics of the system:^{20,21} τ_1 characterizes the thermal coupling between the sample and its surroundings; τ_2 characterizes the thermal relaxation within the sample and is determined by the thermal diffusivity D , and thickness of the sample d . For a heating signal of the form $P = P_0 e^{i\omega t}$ and under the conditions that $(\omega\tau_1)^2 \gg 1$, and $(\omega\tau_2)^2 \ll 1$ the amplitude of the ac temperature oscillations, ΔT_{ac} , is

$$\Delta T_{ac} \approx \frac{P_0}{\omega C} \left(1 - \frac{1}{2(\omega\tau_1)^2} - \frac{(\omega\tau_2)^2}{72} - \frac{\tau_2^2}{72\tau_1^2} \right), \quad (3)$$

where $\tau_1 = C/K$ and $\tau_2 = d^2/D$. For a sufficiently thin sample the heating frequency can be chosen so that the difference between the bracketed quantity in Eq. (3) and 1 is less than 0.1%.

If the sample is not heated uniformly then one has to consider the lateral heat flow in the sample. For this purpose let us assume that the sample is infinite in the x, y plane and a strip of the sample from $x=0$ to $x=a$ is not heated. Then the amplitude of the ac oscillation in the heated part of the sample for $x > a$, $\Delta T(x)_{ac}$, is²⁰

$$\Delta T(x)_{ac} \approx \Delta T_{ac} [1 - \sinh(a/L)e^{-x/L}], \quad (4)$$

where $L = (D/\omega)^{1/2}$ is the thermal diffusion length and ΔT_{ac} is given by Eq. (3). For typical experimental conditions the lateral dimensions of the sample are much bigger than the thermal diffusion length and the correction term for a temperature probe placed in the center of the sample is very small (for our sample it is of the order of 10^{-4}). The temperature probe senses the average ac temperature oscillations within the radius of the thermal diffusion length, the amplitude of which is determined by the local heating power and the heat capacity of the sample per unit of the sample surface area. Knowing the power density and the sample surface area one can calculate the total absolute heat capacity value from Eq. (2). However, the heater coverage determination may be inaccurate, and only a rough estimate of the absolute heat capacity of the sample can be obtained by this method.

A much better way to calibrate data from ac calorimetry is by using the relaxation time method.

III. RELAXATION TIME METHOD

In this method, the heat sink temperature is stabilized at temperature T_0 . The sample is heated at power P , increasing the temperature of the thermometer-sample assembly to $T_0 + \Delta T$, where $\Delta T = P/K$. The sample heater is then turned off, and the sample temperature T relaxes exponentially to T_0 .

$$T(t) = T_0 + \Delta T e^{-t/\tau}, \quad (5)$$

with the time constant

$$\tau = C/K. \quad (6)$$

This simple model gives good results in many cases, but if the thermal conductance of either the sample or the sample-substrate bond is comparable to that of the heat leak or if the heat capacity of the connection wires is appreciable, $T(t)$ must be represented by a more complicated sum of exponentials with different time constants.²² If the ratio τ_2/τ_1 of the time constants defined in the previous section is of the order of 10^{-2} or smaller then Eq. (6) is a reasonable approximation.

Near a phase transition the heat capacity changes rapidly and the decay becomes more complicated and one has to consider the fuller equation:

$$\frac{\dot{T}}{T - T_0} = -\frac{K}{C(T)}, \quad (7)$$

from which Eq. (5) was derived, i.e., near transitions, both T and also its time derivative \dot{T} must be known. This is a principal source of error in this method and the source of its basic limitation for studies of phase transitions. However, the relaxation time method can be used for accurate absolute heat capacity measurements away from the phase transition (to $\sim 2\%$) and it is a very convenient way to calibrate ac calorimetry data.²³

IV. THE CRYOSTAT AND THE SAMPLE ASSEMBLY

The immersion cryostat, shown schematically in Fig. 2, had two chambers (V_1 and V_2 in Fig. 2), which could be evacuated separately. This design allowed either chamber to be filled with exchange gas. The sample assembly was made of copper and consisted of three parts: the adiabatic shield, the sample holder, and the heat sink.

The heat sink, constructed of a thick-walled copper cylinder, was silver soldered to the thin-walled stainless-steel tube which also supported the inner vacuum can. All the electrical leads were carried out through the tube and sealed at two electrical feedthroughs. The adiabatic shield and the sample holder were connected to the heat sink with threaded joints that could be easily disassembled. The adiabatic shield did not have a separate heater but it was thermally well coupled to the heat sink and its function, together with the helium exchange gas, was to minimize temperature gradients around the sample.

A platinum resistance thermometer (Lake Shore Cryotronics, Pt-103, 100Ω at $T=273 \text{ K}$) was inserted into a hole in the sample holder (held in place with Apiezon T vacuum grease; T was selected over Apiezon M and N because it has the highest operating temperature²⁴). There was also an extra hole drilled in the sample holder to accommodate the reference junction of a thermocouple if one was used as a temperature sensor.

The sample was suspended from the sample holder with the sample heater and thinistor leads squeezed between two plastic rings screwed to the sample holder. The leads were soldered to extension leads with thermal-free

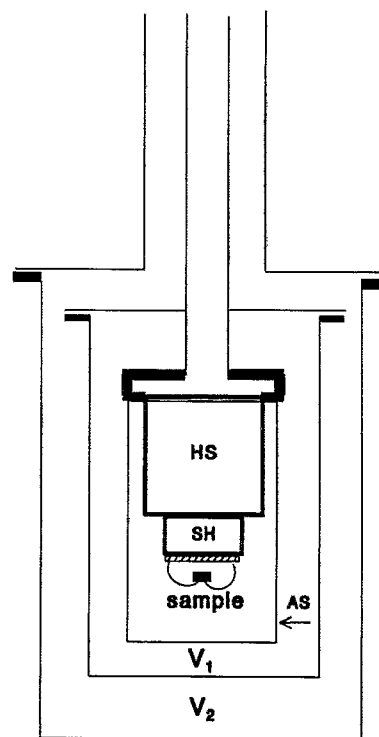


FIG. 2. Schematic of the cryostat and the sample assembly. (AS) adiabatic shield; (HS) heat sink; (SH) sample holder; (S) sample; (V_1, V_2) vacuum chambers.

solder (Leeds and Northrup), at the wall of the sample holder. All extension leads were double-silk wound 38 SWG copper wire. The heat sink heater was made of approximately 2 m of double-silk wound 38 SWG manganin wire ($25 \Omega/\text{m}$ resistance) wound bifilarly around the heat sink and vanished into place with GE-7031 varnish. The temperature stability at the heat sink was within $\pm 1 \text{ mK}$.

We chose electrical heating over chopped light as the heat source because the latter would not allow determination of the total power dissipated in the sample and because it was easier to stabilize the frequency and power of an electrical signal. The resistance heater for the sample must be electrically and mechanically stable on thermal cycling; it should be in good thermal contact with the sample; its heat capacity should be small compared to that of the sample. After other prototypes proved unsuccessful [0.003-mm Mylar foil coated on one side with $0.1\text{-}\mu\text{m}$ -thick layer of manganese did not adhere well to the sample or the leads; Schwartz's method²⁵ of painting a piece of a Mylar foil with graphite suspension gave such a thick heater (around 0.04 mm) that it would make the internal relaxation time of the sample assembly too long], a sample heater was made successfully by evaporating a layer of bismuth on a sample surface insulated with GE-7031 varnish diluted with a 50:50 toluene:ethanol solution. The contacts to the heater were made with $20\text{-}\mu\text{m}$ -diam copper wire. The wires were glued across the sample and close to its opposite edges with silver-loaded epoxy. The bismuth layer was evaporated on the sample after making the contacts and its thickness defined the resistance of the heater, around 50Ω . The

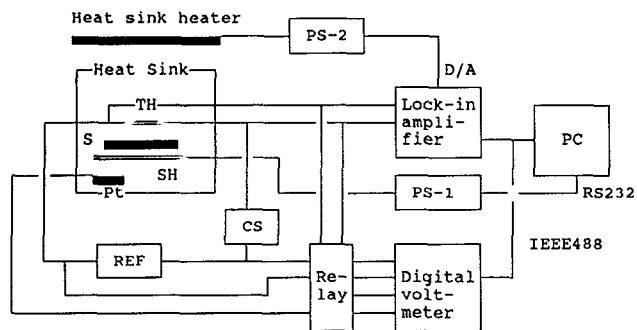


FIG. 3. Block diagram of the automated ac calorimeter. (PC) personal computer; (RS232) serial interface; (IEEE488) parallel interface; (PS-1 and PS-2) power supplies; (D/A) digital-to-analog outputs of the lock-in amplifier; (CS) current source; (REF) reference resistor; (Pt) platinum resistance thermometer; (SH) sample heater; (S) sample; (TH) thinistor.

total thickness of the heater (GE varnish and bismuth layer) was around $4 \mu\text{m}$ and it accounted for about 5% of the total heat capacity. Heaters made as described here were very reliable: they were in good thermal contact with the sample and did not change their resistance over time or heat treatment.

The temperature sensor was a thinistor (thick film flake thermistor from Victory Engineering Corporation, symbol 53K1A500, $250 \text{ k}\Omega \pm 20\%$ zero power resistance at 25°C , dimensions $0.5 \times 0.5 \times 0.04 \text{ mm}^3$). The thinistor was glued to the sample on the surface opposite to the heater.

V. ELECTRONIC INSTRUMENTATION AND DATA ACQUISITION SYSTEM

A. Heater power circuit

Unwanted fluctuations of heater power and frequency could be mistaken for changes in heat capacity, reducing the sensitivity of the calorimeter. This was avoided here with a programmable microprocessor-controlled power supply (PS-1 in Fig. 3), designed to provide a constant heating power although the heater resistance is temperature dependent. The heating power requirement was very small ($< 0.5 \text{ mW}$). An additional requirement was that this heating power be applied as a low-frequency sine wave, with a stable, programmable frequency. Since a microprocessor was employed in the design, the sine wave synthesis was software generated.

In use, the operator would send the controller the following parameters, *via* an RS-232 serial data link from the host PC computer: frequency (resolution 0.01 Hz); desired heater power; approximate sample resistance (at that temperature). Using the input power and resistance values, an approximate heating voltage was derived, and a sine wave of this voltage was generated using a dual 12-bit DAC. One half of this DAC was used to provide a dc voltage with an amplitude equal to the peak value of the sine wave. The output of the second half of the DAC was a unipolar signal with a sine waveform. By mixing in the signal from the first DAC, at a ratio of 0.5, a true sine wave signal centered at 0 V was derived. This sine wave was buffered and applied

to the sample in a feedback arrangement using two wires to apply heater power, and two wires to sense the voltage at the sample.

A $50\text{-}\Omega$ precision resistor was placed in series with the sample to sense the current. The voltage over this resistor was amplified and sent to a SAMPLE/HOLD circuit and the microprocessor placed this circuit in the HOLD mode at the peak of the heater signal. This circuit provided an accurate alternative to rectifying or phase-detecting the heater current ac signal since those methods require an output filter, which at the low excitation frequency used, would result in a very slow response time. The dc voltage provided by the SAMPLE/HOLD was fed to a synchronized voltage-to-frequency converter. The output pulse-train frequency was measured by the microprocessor. The microprocessor was programmed to stay in a loop measuring heater current, forming the voltage-current product, and "fine-tuning" the heater excitation voltage until the requested power was reached. Each iteration of the loop took $\sim 3 \text{ s}$.

At any time the host PC could interrogate the microprocessor, through the RS-232 link, to determine the present heater voltage and current. Alternately, a new power level or excitation frequency could be specified.

B. Sample temperature measurement

The amplitude and phase of the temperature oscillation at the sample were measured by a Stanford Research 530 lock-in amplifier using the thinistor as a temperature sensor (TH in Fig. 3). The current to the thinistor was supplied by a very stable current source (CS in Figs. 3 and 4) also built for the purposes of this project. A Hewlett Packard 3456A digital voltmeter measured the resistance of the thinistor in the resistance ratio mode to give the absolute temperature of the sample. The reference high-precision resistor (two connected in series; VHA518-7 $100\text{-k}\Omega$ resistors from Vishay Resistive Systems Group, tolerance 0.001% , temperature coefficient $\pm 1.5 \text{ ppm/K}$ around room temperature) was embedded in a temperature-regulated aluminum block (REF in Fig. 3). This block was heated to a relatively constant ($\pm 1 \text{ K}$) above-ambient temperature, by a simple transistor pass regulator driving two $100\text{-}\Omega$, 1-W resistors imbedded in the isothermal block (Fig. 4). A solid-state temperature controller IC was used in an initial design, but was removed when it was found that its switching transients, which occurred around the setpoint temperature, were affecting the constant current source, even though the two circuits were powered from separate supplies.

C. Constant current source

The thinistor current was $6.95 \mu\text{A}$. The constant current was based on a small reference IC (National Semiconductor LM399, temperature coefficient $\sim 30 \text{ ppm/K}$) in an insulated can package, which contained both a 6.95-V reference and a small temperature-controlled heater, all on the same substrate. Its internal temperature was stabilized above the ambient temperature.

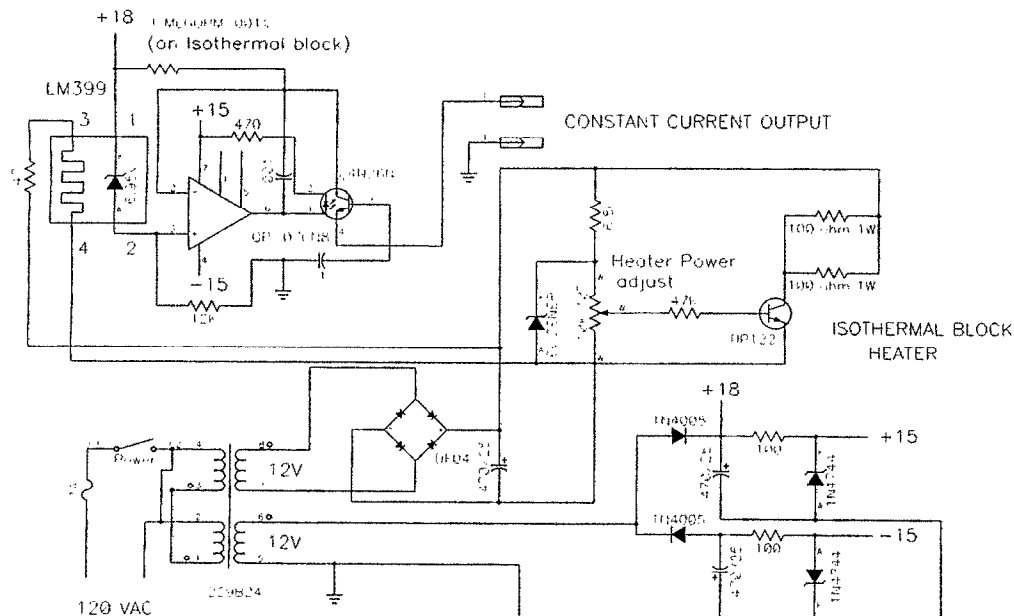


FIG. 4. Constant current source.

A constant current was generated by passing 18 V through a 1-M Ω standard resistor (VHA518-10 made by Vishay, tolerance 0.001%, temperature coefficient ± 1.5 ppm/K, also mounted in the aluminum block), a pass element, and then through the external thinistor-reference resistor circuit to ground. The voltage drop across 1 M Ω , at 6.95 μ A, was 6.95 V, the same value as that of the LM399 voltage reference. An operational amplifier was used to compare these voltages and its output was passed through a 4N26N optocoupler's light-emitting diode. The connection between the operational amplifier and optocoupler was such that if the output current was less than 6.95 μ A, the output of the operational amplifier would tend to go negative, causing an increased current through the infrared LED in the optocoupler. This would cause the 4N26N phototransistor to pass more current, increasing the current output until equilibrium was reached at 6.95 μ A. More conventional circuits were tried but were found to be prone to modulation by the low-frequency heater signal and/or noise that could not be eliminated by RC filtering of the current source, as this introduced large amplitude and phase errors in the measurement of the temperature oscillation by the lock-in amplifier. Amplitude and phase errors in the signal measurement were minimized by isolating the highly sensitive operational amplifier input terminals from the thinistor/reference resistor.

The power supplied to the heat sink heater was controlled by the buffered and amplified DAC outputs of the lock-in amplifier (Fig. 5 and PS-2 in Fig. 3) which allowed for coarse (DACX5) and fine (DACX6) heat adjustments.

The heat sink temperature was measured with the platinum resistance thermometer (Pt in Fig. 3) by the 3456 DVM in four-wire resistance mode with thermal emf compensation. The relay switched the 3456 DVM between

measuring the resistance of the Pt thermometer and the ratio measurement.

The DVM and the lock-in amplifier were interfaced with an IBM-compatible, 386 class computer by an IEEE-488 parallel data link. All the operations associated with the control of the electronics, temperature control, and data acquisition were performed by the computer.

VI. TEST MEASUREMENTS: HEAT CAPACITY OF GADOLINIUM

A. Thermometry

The temperature scale used in this experiment was based on the resistance of the platinum thermometer, converted to temperature using the Chebychev polynomial calibration equations provided by the manufacturer. In the temperature range of the experiment the rms error of the fit was around 5 mK.

The sample temperature and the ac temperature oscillations were measured with the thinistor mounted on the sample. The thinistor was calibrated against the Pt thermometer every 0.5 K while the temperature was increased linearly at a rate of a few mK per minute (the inside of the calorimeter was filled with He exchange gas). The simple polynomial,

$$T = A + B \ln R + C (\ln R)^2,$$

was fit to the calibration data by a least-squares procedure, giving a random scatter of ~ 30 mK over the temperature interval of the measurements. We chose to use Eq. (8) over other functions²⁶ because of its simplicity and its linearity in the parameters. For the purpose of converting lock-in amplifier readings to temperature we also had to find the inverse fit, i.e., $\ln R = f(T)$, and calculate ΔT for small ΔR by differentiation of Eq. (8).

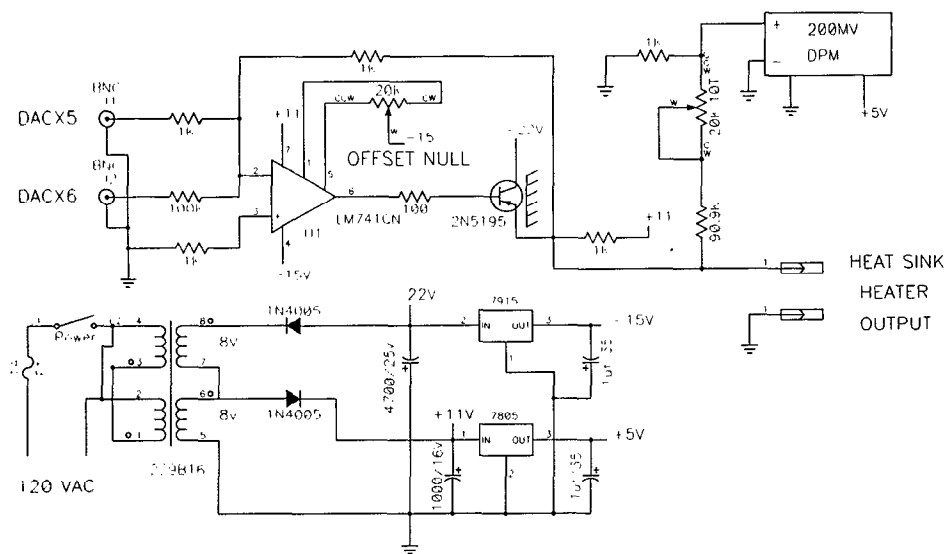


FIG. 5. Heat sink heater control circuit.

The thinistor calibration was repeated periodically. When the thinistor was thermally cycled from 360 K down to liquid-nitrogen temperature its calibration shifted towards lower temperature by about 200 mK. Over a few months, values tended to give higher temperatures for a given thinistor resistance when the thinistor was kept in vacuum or in a helium atmosphere, which may indicate slow degradation of the thinistor, but results were within 150 mK. Most important, the sensitivity [resistance derivative of Eq. (8)] was constant for different calibrations in the temperature range from 220 to 330 K. The temperature coefficient of the resistance of the thinistor, $\alpha = \delta \ln R / \delta T$, decreased with temperature from a room-temperature value of around 4.6% resistance change/K. Thermistors are among the most sensitive thermometers; they are much more sensitive than thermocouples commonly used in ac calorimeters. The value of α obtained for the thinistor used here is typical for high-sensitivity bead (glass encapsulated) thermistors. However, the thinistor is a superior temperature detector in an ac calorimetry experiment because it combines a high sensitivity with a very low thermal mass and it can be placed in very good thermal contact with a sample. A thermistor similar to the one used here also can be used successfully around the liquid-nitrogen temperature⁶ provided that it is not thermally cycled to room temperature.

The temperature of the experiment was scanned linearly up or down by regulating the power to the heat sink. It was done by the computer which changed the voltage at the analog outputs of the lock-in amplifier (Sec. V) so as to induce the preset temperature drift rate.

The design of this calorimeter allows its operation in the temperature range up to the melting point of the indium seals. The lower range of temperature is limited by the platinum resistance thermometer, which loses sensitivity below about 10 K.

B. Sample

Gadolinium (Gd) is one of the rare-earth metals and it exhibits a ferromagnetic phase transition at 292 K.²⁷ The critical behavior of gadolinium is not yet fully understood:²⁸ static critical exponent measurements span predictions of Heisenberg and Ising critical behaviors.²⁷ It has been suggested by Geldart *et al.*²⁹ that the critical behavior close to T_c may be dominated by magnetic dipole-dipole interactions and in the reduced temperature range $10^{-5} < t < 10^{-3}$ the heat capacity of Gd should be described by Landau theory with logarithmic corrections. In order to test this theory, our objective was to obtain high-resolution heat capacity data on Gd near its ferromagnetic phase transition. Gadolinium is also a good candidate for testing a high-resolution calorimeter because there is ample experimental data available on the heat capacity of gadolinium around its Curie point from adiabatic calorimetry,^{30,31} differential scanning calorimetry,³² ac calorimetry,³³⁻³⁵ and continuous heating.³⁶

The sample of Gd used in the present study was cut from an electrotransport-purified single crystal of Gd grown at the Ames Laboratory, Energy and Mineral Resources Institute. This crystal has been characterized by previous resistivity²⁸ [$R(293 \text{ K})/R(4.2 \text{ K}) \approx 150$] and magnetic susceptibility³⁷ studies. The sample (final dimensions $3.08 \times 5.18 \times 0.12 \text{ mm}^3$) was ground to a thickness of 0.12 mm by rubbing against a silicon carbide 600 grit grinding paper, and then it was polished with diamond paste. Afterwards the sample was annealed at 850 °C for 24 h in a vacuum of 5×10^{-6} Torr in a tantalum foil wrap. A heater was evaporated on one side of the sample (Sec. IV) and a thinistor was attached with GE-7031 varnish to the center of the opposite side. The thinistor extension leads, made of two pieces of platinum wire 17 μm in diameter, were soldered to the calorimeter extension wires. The total mass of the thinistor and platinum wires was 0.4 mg (Gd mass: 0.0113 g; sample assembly mass: 0.0120 g).

C. Measurement in the ac mode

The optimum range for the frequency of the heating signal was found by measuring the amplitude of the ac temperature oscillations, ΔT_{ac} , as a function of the heating frequency, ω . For heating frequencies in the range from 1 to 3.5 Hz, ΔT_{ac} was proportional to ω^{-1} and the phase shift between the heating signal and the ac oscillations was around 1° . The phase shift was almost zero and changed the least over the phase transition for a heating frequency of around 1.9 Hz. In a typical measurement run the sample was heated with a signal of frequency of 1.9 Hz and rms power of a few hundreds of μW ; this induced temperature oscillations of the order of a few mK resulting in voltage oscillations over the thinistor of a few hundreds of μV . The voltage signal of this order was easily detected by the lock-in amplifier and was free of any visible noise.

The temperature of the heat sink was increased or decreased at a rate of a few mK per minute and the voltage oscillation amplitude and the heat sink temperature were recorded as functions of time. The sample temperature was derived from the heat sink temperature and the constant temperature difference between the sample and the heat sink, ΔT_{dc} . ΔT_{dc} , which depended on the sample heating power, the pressure of He exchange gas, and the rate of temperature change, was measured with the thinistor at the beginning and the end of each run; it changed by at most 100 mK during a single run lasting more than 24 h, and for the purpose of data analysis it was assumed to be a linear function of temperature.

During measurement the inside of the calorimeter was filled with 2×10^{-3} Torr of helium gas. At this pressure the leads contributed approximately 30% to the total heat conductance. The experimentally measured external time constant for this pressure, τ_2 , was around 3.5 s; the internal time constant τ_1 was estimated to be of the order of 10^{-3} s.

Measurements made at different pressures of helium (2×10^{-3} Torr to atmospheric pressure) and also when the inside chamber was evacuated (to 5×10^{-6} Torr) gave the same heat capacity results. Increasing the temperature drift rate from 5 to 60 mK/min also did not affect the results. This leads us to believe that the sample was in thermal equilibrium during the measurements reported here.

The results of a typical measurement series on Gd are shown in Figs. 6 and 7. The data points were collected every 100 mK away from the critical temperature, and every 10 mK close to the critical temperature. The temperature was increased at a rate of around 5 mK per minute and ΔT_{ac} was in the range 2.5–3.5 mK.

The only tabulated data for the heat capacity of Gd values are those of Griffel *et al.*,³⁰ their values also are plotted in Fig. 6 for comparison. Our data match very well the data of Griffel *et al.* on the low-temperature side of the transition but there is a slight difference in the heat capacity values on the high-temperature side of the transition. This likely is due to differences in sample quality. (The main features of heat capacity curves over the Curie point in Gd, as reported by different authors, are their differences in Curie temperatures, the degree of rounding at T_c , the relative differences in heat capacities for the ferromagnetic

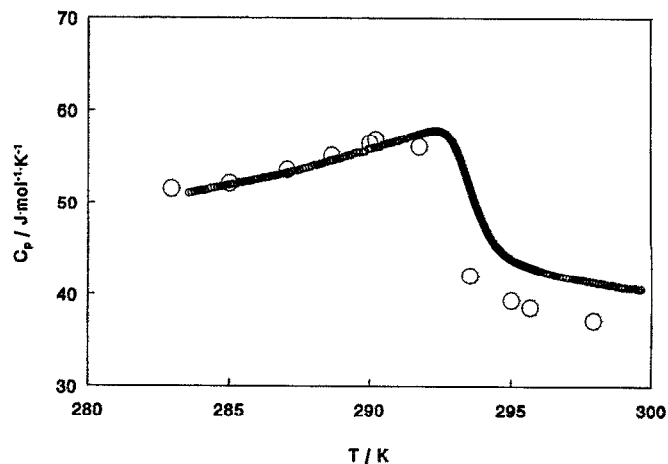


FIG. 6. The heat capacity of Gd near its ferromagnetic phase transition; large circles denote the heat capacity data of Griffel *et al.* (Ref. 30).

to paramagnetic regions, and the peak value of the heat capacity, and these features seem to depend on the degree of impurities in the sample and its annealed or nonannealed state.^{32–36} We are currently making further heat capacity measurements on Gd to investigate the influence of the sample preparation procedure on the shape of the heat capacity anomaly at the phase transition and a fuller analysis of the results will be published elsewhere.)

The scatter of our data points is around 0.2%. Based on the literature data, the resolution of these data is one of the highest reported to date for ac calorimetry and other calorimetric methods. In addition, this is the first report of high-resolution data on heat capacity of Gd, measured by the ac method and calibrated with absolute heat capacity measurements made on the same sample (*vide infra*).

D. Measurement in the relaxation mode

The heat capacity data obtained by ac calorimetry were normalized to the absolute heat capacity data collected in the relaxation mode. In this mode we measured

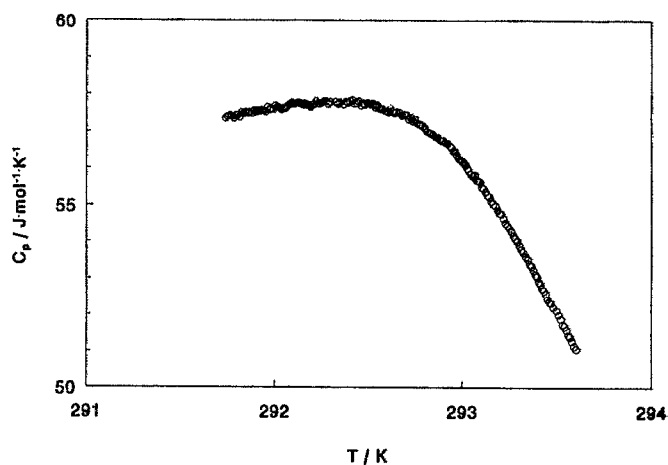


FIG. 7. The heat capacity of Gd in the proximity of the critical temperature.

TABLE I. The experimental heat capacities of Gd obtained by the relaxation method, in order of determination.

T/K	$C_p / (\text{J K}^{-1} \text{mol}^{-1})$
284.1	51.45
285.1	51.59
286.1	51.86
297.1	39.95
298.1	39.27
299.1	39.13
285.2	52.29
286.1	52.00
286.2	52.49

the heat capacity of the sample below the phase transition in the temperature range from 284 to 287 K, above the phase transition at 298 and 299 K, and then again below the phase transition to check for thermal hysteresis effects.

The measurement procedure was as follows. The temperature of the heat sink was stabilized and the temperature difference between the sample and the heat sink, ΔT , was measured as a function of the sample heating power P . The maximum temperature difference ΔT_{max} was around 300 mK. The thermal conductance was calculated from $P(\Delta T)$. In the next step the sample temperature was raised to ΔT_{max} , then the heater was turned off, and the sample temperature was recorded as a function of time (at a rate of around ten temperature readings per second). The last step was repeated several times. The thermal relaxation time was found by a least-squares fit to the temperature decay data with an exponential function [see Eq. (5)], and the sample heat capacity at $(T + \Delta T_{\text{max}}/2)$ was calculated from Eq. (6). The precision of the measurement, as estimated from the standard deviations of the fits, is within 2%.

The heat capacity values used to calibrate the data in Figs. 6 and 7 are listed in Table I. The data in the table were corrected for the heat capacities of the addenda using literature values for the heat capacity of silver-loaded epoxy³⁸ and copper.³⁹ These correction terms contributed around 10% to the total heat capacity of the sample assembly. The data were not corrected for the heat capacities of the GE varnish, bismuth layer, or the thinistor assembly since their combined mass was less than 1% of the total sample assembly.

VII. DISCUSSION

The sensitivity of an ac calorimeter is limited by the accuracy of the measurement electronics, the stability of thermal regulation, and by various thermodynamic noises, e.g., the Johnson noise in the thermometer, the $1/f$ noise, noise in the lock-in amplifier, and pick-up noise. (See Kenny and Richards¹⁶ for a discussion of the performance of an ideal ac calorimeter.) The major source of noise in our experiment is the $1/f$ noise. We measured the noise density using the noise-measurement capability of the lock-in amplifier, and found that it varied almost as $1/f$ in the frequency range from 1 to 10 Hz. The noise contribution to the measured signal was around $0.5 \mu\text{V}$ (around 0.2% of

the total signal) for integration times typically used in our experiment (10 s), in good agreement with our calculated estimates of the $1/f$ noise in the thinistor, and with the observed scatter in our data. This sets a lower limit on the resolvable change in ΔT_{ac} as 10^{-5} K. The Johnson noise in the thinistor is around 10% of the thinistor $1/f$ noise.

Similar values for ac calorimeter sensitivity are given by Garland¹⁴ for a room-temperature experiment employing a microbead thermistor as a temperature oscillation detector. The sensitivity of our measurement could be improved significantly by further thinning the sample and operating at higher heating frequency.

Despite its relatively simple mechanical and electronic construction, our calorimeter compares well with other high-resolution ac calorimeters.^{14,16,17,40} We were able to highly resolve a useful temperature signal without the expensive addition of a good-quality ac bridge. This was achieved by using a very stable current source and a miniature and very sensitive temperature detector. The simple temperature control system was based on two D/A outputs of the lock-in amplifier which better utilized the capabilities of this instrument and made computer control of the temperature drift rate relatively easy. To our knowledge this microprocessor-controlled sample heater is the first attempt to provide a constant and known oscillatory heat input to a sample by accounting for the temperature dependence of the heater resistance. This heater made it possible not only to highly resolve the heat capacity of the sample but also to measure its absolute heat capacity. This is especially important in the light of the fact that heat capacity changes over a phase transition depend very much on sample quality and many other ill-defined factors, so reference to the literature for data calibration often seems unwarranted.

ACKNOWLEDGMENTS

The authors thank R. Conrad for machining this calorimeter, D. McLean, B. Fullerton, and R. Dunlap for technical assistance and the Natural Sciences and Engineering Research Council of Canada (for grants to MAW) and the Killam Fund (for a scholarship to GB).

Note: A detailed drawing of the electronic system has been deposited with AIP's Physics Auxiliary Publication Service (PAPS) (see Ref. 41).

¹E. F. Westrum, Jr., G. T. Furukawa, and J. P. McCullough, in *Experimental Thermodynamics*, edited by J. P. McCullough and D. W. Scott (Butterworth, London, 1968), Vol. 1.

²K. G. Wilson, *Phys. Rev. B* **4**, 3174 (1971); *Rev. Mod. Phys.* **47**, 773 (1975).

³A. D. Bruce, *Adv. Phys.* **29**, 111 (1980).

⁴A. R. Chowdhury, G. S. Collins, and Ch. Hohenemser, *Phys. Rev. B* **30**, 6277 (1984).

⁵E. Gmelin, *Thermochim. Acta* **29**, 1 (1979).

⁶G. Ahlers, A. Kornblit, and H. J. Guggenheim, *Phys. Rev. Lett.* **34**, 1227 (1975).

⁷R. N. Dixit, S. M. Pattalwar, S. Y. Shete, and B. K. Basu, *Rev. Sci. Instrum.* **60**, 1351 (1989).

⁸M. A. White, *Thermochim. Acta* **74**, 55 (1984).

⁹W. Hemminger and G. Höhne, *Calorimetry. Fundamentals and Practise* (Verlag Chemie, Weinheim, 1984).

- ¹⁰M. J. Buckingham, C. Edwards, and J. A. Lipa, *Rev. Sci. Instrum.* **44**, 1167 (1973).
- ¹¹R. E. Schwall, R. E. Howard, and G. R. Stewart, *Rev. Sci. Instrum.* **46**, 1054 (1975).
- ¹²P. F. Sullivan and G. Seidel, *Phys. Rev.* **173**, 679 (1968).
- ¹³D. L. Connelly, J. S. Loomis, and D. E. Mapother, *Phys. Rev. B* **3**, 924 (1971).
- ¹⁴C. W. Garland, *Thermochim. Acta* **88**, 127 (1985).
- ¹⁵S. Imaizumi, K. Suzuki, and I. Hatta, *Rev. Sci. Instrum.* **54**, 1180 (1983).
- ¹⁶T. W. Kenny and P. L. Richards, *Rev. Sci. Instrum.* **61**, 822 (1990).
- ¹⁷G. M. Schmiedeshoff, N. A. Fortune, J. S. Brooks, and G. R. Stewart, *Rev. Sci. Instrum.* **58**, 1743 (1987).
- ¹⁸J. D. Baloga and C. W. Garland, *Rev. Sci. Instrum.* **48**, 105 (1977).
- ¹⁹P. Schwartz, *Phys. Rev. B* **4**, 920 (1971).
- ²⁰P. R. Garnier, Ph. D. thesis, University of Illinois at Urbana-Champaign, 1972.
- ²¹D. S. Simons, Ph. D. thesis, University of Illinois at Urbana-Champaign, 1973.
- ²²J. P. Shepherd, *Rev. Sci. Instrum.* **56**, 273 (1985).
- ²³G. R. Stewart, *Rev. Sci. Instrum.* **54**, 1 (1983).
- ²⁴A. J. Gordon and R. A. Ford, *The Chemist's Companion: A Handbook of Practical Data, Techniques, and References* (Wiley, New York, 1972).
- ²⁵P. M. Schwartz, Ph. D. thesis, University of Illinois, 1969.
- ²⁶G. Bosson, F. Gutmann, and L. M. Simmons, *J. Appl. Phys.* **21**, 1267 (1950).
- ²⁷A. R. Chowdhury, G. S. Collins, and Ch. Hohenemser, *Phys. Rev. B* **33**, 6231 (1986).
- ²⁸D. J. W. Geldart, K. De'Bell, J. Cook, and M. J. Laubitz, *Phys. Rev. B* **35**, 8876 (1987).
- ²⁹D. J. W. Geldart, P. Hargraves, N. M. Fujiki, and R. A. Dunlap, *Phys. Rev. Lett.* **62**, 2728 (1989).
- ³⁰M. Griffel, R. E. Skochdopole, and F. H. Spedding, *Phys. Rev.* **93**, 657 (1954).
- ³¹A. V. Voronel, S. R. Garber, A. P. Simkina, and I. A. Charkina, *Sov. Phys. JETP* **22**, 301 (1966).
- ³²L. B. Robinson and F. Milstein, *Solid State Commun.* **13**, 97 (1973).
- ³³E. S. Lewis, *Phys. Rev. B* **1**, 4368 (1970).
- ³⁴D. S. Simons and M. B. Salamon, *Phys. Rev. B* **10**, 4680 (1974).
- ³⁵G. H. J. Wantenaar, S. J. Campbell, D. H. Chaplin, and G. V. H. Wilson, *J. Phys. E* **10**, 825 (1977).
- ³⁶P. C. Lanchester, K. Robinson, D. P. Baker, I. S. Williams, R. Street, E. S. R. Gopal, *J. Magn. Magn. Mater.* **15-18**, 461 (1980).
- ³⁷P. Hargraves, R. A. Dunlap, D. J. W. Geldart, and S. P. Ritcey, *Phys. Rev. B* **38**, 2862 (1988).
- ³⁸A. Berton, J. Chaussy, J. Ocin, and B. Souletie, *Cryogenics* **17**, 584 (1977).
- ³⁹R. Hultgren, R. L. Orr, P. D. Anderson, and K. K. Kelley, *Selected Values of Thermodynamic Properties of Metals and Alloys* (Wiley, New York, 1963).
- ⁴⁰J. M. Viner, D. Lamey, C. C. Huang, R. Pindak, and J. W. Goodby, *Phys. Rev. A* **28**, 2433 (1983).
- ⁴¹See AIP document No. RSINA-63-3944-1 for 1 page of a detailed drawing of the electronic system. Order by PAPS number and journal reference from American Institute of Physics, Physics Auxiliary Publication Service, 335 East 45th Street, New York, NY 10017. The price is \$1.50 for each microfiche (60 pages) or \$5.00 for photocopies of up to 30 pages, and \$0.15 for each additional page over 30 pages. Airmail additional. Make checks payable to the American Institute of Physics.

Review of Scientific Instruments is copyrighted by the American Institute of Physics (AIP). Redistribution of journal material is subject to the AIP online journal license and/or AIP copyright. For more information, see <http://ojps.aip.org/rsio/rsicr.jsp>
Copyright of Review of Scientific Instruments is the property of American Institute of Physics and its content may not be copied or emailed to multiple sites or posted to a listserv without the copyright holder's express written permission. However, users may print, download, or email articles for individual use.